

ESTIMATING THE PROBABILITY OF VOLCANIC DISRUPTION OF THE CANDIDATE YUCCA MOUNTAIN REPOSITORY USING SPATIALLY AND TEMPORALLY NONHOMOGENEOUS POISSON MODELS

Charles B. Connor and Brittain E. Hill
 Center for Nuclear Waste Regulatory Analyses
 Southwest Research Institute
 6220 Culebra Road, San Antonio, Texas, 78228-0510, USA
 210-522-5160

ABSTRACT

The candidate high-level nuclear waste repository site at Yucca Mountain, Nevada, is located near Quaternary basaltic volcanoes. The probability of volcanic disruption of the candidate repository site during the next 10,000 years must be determined to evaluate the risks associated with basaltic volcanism. Our estimate of Quaternary recurrence rates in the Yucca Mountain region is 7 ± 3 volcanoes per million years (v/my), which reflects the uncertainties present in the ages of Quaternary cinder cones. Application of Clark-Evans and Hopkins F-tests indicates that the locations of Quaternary and Neogene basaltic volcanoes near the proposed repository site are not adequately described by a homogeneous Poisson distribution because mafic volcanoes in the Yucca Mountain area cluster. Nonhomogeneous Poisson models using six to seven near-neighbor volcanoes result in regional recurrence rates that are within the range of calculated Quaternary recurrence rates. Probabilities for disruption of a repository area calculated using a range of Quaternary recurrence rates vary from 8.0×10^{-5} to 3.4×10^{-4} for a 10,000 year period, with most estimates between 1×10^{-4} and 3×10^{-4} . Spatially nonhomogeneous Poisson models using ten to eleven near neighbors produce recurrence rates comparable to average rates of basaltic volcanism since the cessation of Miocene silicic volcanism (≈ 3 v/my) and disruption probabilities of 6.9×10^{-5} to 9.2×10^{-5} .

INTRODUCTION

Volcanic eruptions at or adjacent to the candidate high-level waste (HLW) repository could potentially result in release of HLW into the accessible environment. Determining the probability of a volcanic eruption in the repository area is thus a critical step in the evaluation of potential risks associated with the Yucca Mountain site. The objective of this paper is to present a range of probability models that take into account some of the temporal and spatial controls on Quaternary mafic volcanoes in the Yucca Mountain region (YMR).

Basaltic volcanism has been a characteristic of the YMR since about 11 Ma.¹ The preserved volcanic units represent the eruption of at least 40 km^3 of generally alkaline basalt, with volumes of individual centers ranging from >10 to $<0.1 \text{ km}^3$.¹⁻² Basaltic volcanoes in the region represent a variety of eruption styles, and range from relatively low explosivity effusions of lava flows and small-volume cinder cones, to highly explosive phreatomagmatic eruptions.³ Although each eruptive style will impact the repository differently, any type of mafic eruption within or adjacent to the repository would adversely affect repository performance.^{1,4} The focus of this

paper is to estimate the probability of mafic volcanic activity within or adjacent to the repository during the next 10,000 years, through the application of nonhomogeneous Poisson models.

Figure 1 illustrates the location of mapped and inferred post-caldera basaltic vents in the YMR.³ Geographic information and estimated age of initial eruptive activity at each center are summarized in Table 1. Dated basaltic vents vary in age from approximately 10 Ma for the Paiute Mesa basalts to approximately 0.10 Ma for the Lathrop Wells cinder cone.⁵⁻⁶ Various dating methods have yielded estimated ages for Lathrop Wells of between 0.4 and 0.02 Ma.⁷⁻¹⁰ There are relatively few high-precision dates from other cinder cones in the area, so these dates are considered to be estimates.

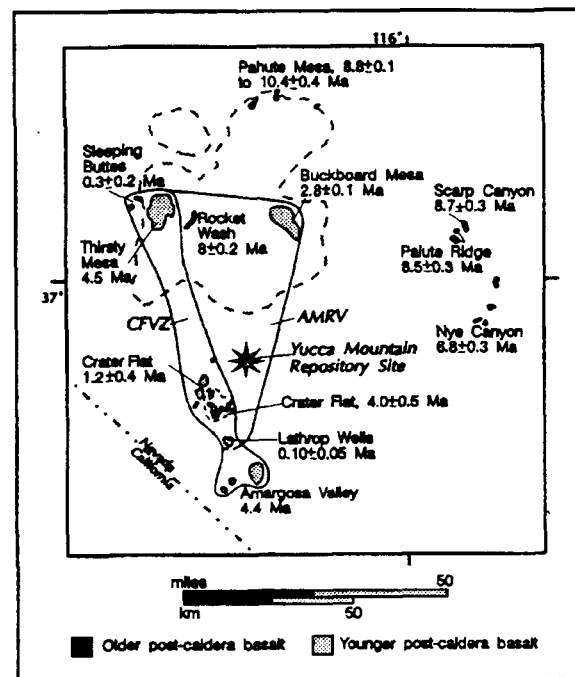


FIGURE 1: Post-caldera basaltic vent locations in the YMR (modified from Crowe³). Basaltic units are shaded by relative age and mean numeric age is posted (Table 1). Miocene calderas of the Timber Mountain caldera complex (dashed lines) and HLW repository (star) are shown.

YMR RECURRENCE RATES FOR VOLCANO FORMATION

All probability models proposed to date rely on estimates of the expected regional recurrence rate of volcanism in the YMR in order to calculate the probability of future disruptive volcanic activity. Most previous estimates of regional recurrence rate are between 1 and 12 volcanoes per million years (v/my).¹¹⁻¹⁵ Ho et al.¹³ and Ho¹² provide several examples of techniques used to estimate regional recurrence rates. The simplest approach is to average the number of events that have occurred during some arbitrary time period. For instance, Ho et al.¹³ average the number of volcanoes that have formed during the Quaternary (1.6 m.y.) to calculate the recurrence rate. Through this approach they estimate an expected recurrence rate of 5 v/my. Crowe et al.⁴ averaged the number of new volcanoes over a 1.8 million year period. Crowe et al.¹⁵ consider the two Little Cones to represent a single magmatic event, and therefore conclude that there are seven Quaternary centers in the region. This lowers the estimated recurrence rate to approximately 4 v/my. The probability of a new volcano forming in the YMR during the next 10,000 yr is between 4% and 5%, assuming a recurrence rate of between 4 and 5 v/my.

An alternative approach to calculating recurrence rate is the repose-time method.¹³ In this method, a recurrence rate is defined using a maximum likelihood estimator that averages events over a specific period of volcanic activity:

$$\lambda = \frac{(E-1)}{(T_o - T_y)} \quad (1)$$

where E is the number of events, T_o is the age of the first event, T_y is the age of the most recent event, and λ is the estimated recurrence rate. Using eight Quaternary volcanoes as the number of events, E , and 0.1 Ma for the formation of Lathrop Wells, the estimated recurrence rate depends on the age of the first Quaternary volcanic eruption in Crater Flat (Figure 1). Using a mean age of 1.2 Ma yields an expected recurrence rate of approximately 7 v/my. However, the ages of Crater Flat volcanoes are currently estimated at 1.2 ± 0.4 Ma. Using the upper and lower bounds of this uncertainty, the expected recurrence rate is between approximately 4.5 and 10 v/my. The repose-time method has distinct advantages over techniques that average over an arbitrary period of time because it restricts the analysis to a time period that is meaningful in terms of volcanic activity. In this sense it is similar to methods applied previously to estimate time-dependent relationships in active volcanic fields.¹⁶ However, because the method depends on the age of the oldest event, uncertainty in volcano ages has a greater effect. In this case, the result is the recurrence rate is known only to within approximately 7 ± 3 v/my.

Ho¹² applied a Weibull-Poisson technique¹⁷ to estimate the recurrence rate of new volcano formation in the YMR as a function of time. Ho¹² estimates $\lambda(t)$ as:

$$\lambda(t) = \left(\frac{\beta}{\theta}\right) \left(\frac{t}{\theta}\right)^{\beta-1} \quad (2)$$

where t is the total time interval under consideration (such as the Quaternary), and β and θ are intensity parameters in the Weibull distribution that depend on the frequency of new volcano formation within the time period, t , and the change in

Table 1. Locations of volcanic centers and ages used for statistical models.¹⁻⁵ Vent coordinates in Universal Transverse Mercator, zone 11, Clarke 1866 spheroid.

Name	Age (Ma)	UTM easting	UTM northing	Name	Age (Ma)	UTM easting	UTM northing
Amargosa Valley SW	≈ 4.4	543376	4048820	Hidden Cone	0.3 ± 0.2	523301	4113698
Amargosa Valley	≈ 4.4	544817	4050859	Thirsty Mesa	≈ 4.5	528129	4112249
Amargosa Valley NE	4.4	550306	4053139	Rocket Wash	8.0 ± 0.2	535539	4109028
Lathrop Wells	0.10 ± 0.05	543737	4060073	Buckboard Mesa	2.8 ± 0.1	554946	4109111
Crater Flat S	4.0 ± 0.5	541493	4066057	Pahute Mesa W	10.4 ± 0.4	548758	4133489
Crater Flat E	4.0 ± 0.5	543704	4067644	Pahute Mesa	9.1 ± 0.7	554170	4134467
Crater Flat W	4.0 ± 0.5	540584	4067787	Pahute Mesa E	8.8 ± 0.1	561927	4132182
Crater Flat NW	4.0 ± 0.5	539915	4070959	Paiute Ridge S	8.5 ± 0.3	593698	4101888
Crater Flat W	4.0 ± 0.5	536879	4068573	Paiute Ridge N	8.5 ± 0.3	593611	4103166
Little Cone SW	1.2 ± 0.4	534626	4069423	Scarp Canyon	8.7 ± 0.3	595625	4103906
Little Cone NE	1.2 ± 0.4	534825	4069884	Nye Canyon N	6.8 ± 0.3	603210	4091744
Red Cone	1.2 ± 0.4	537259	4071648	Nye Canyon	6.8 ± 0.3	602370	4085671
Black Cone	1.2 ± 0.4	538257	4074275	Nye Canyon SE	6.8 ± 0.3	600999	4082470
Northern Cone	1.2 ± 0.4	540088	4079455	Nye Canyon SW	6.8 ± 0.2	599557	4083139
Little Black Peak	0.3 ± 0.2	521298	4111346				

Table 2. Dependence of the Weibull-Poisson model of recurrence rate of volcano formation on age.

Volcano Age Estimates	t(m.y.)	β	θ	λ (v/my) (90% Confidence Interval)	P[10,000 yr]
mean ages ¹	1.6	1.1	0.2	5.4 (1.8, 12.4)	5%
oldest ages ²	1.6	0.3	0.001	1.5 (0.5, 3.44)	1.5%
youngest ages ³	1.6	2.2	0.6	11.0 (3.7, 25.3)	10%
mean ages ¹	1.2	0.3	0.002	2.1 (0.7, 4.8)	2%
varying ages ⁴	1.2	0.7	0.2	4.8 (1.6, 11.0)	5%

- ¹ Volcanoes are assumed to have the mean ages reported in Table 1. For example, an age of 1.2 m.y. is used for Black Cone.
² Volcanoes are assumed to have the oldest ages reported in Table 1. For example, an age of 1.6 m.y. is assumed for Black Cone.
³ Volcanoes are assumed to have the youngest ages reported in Table 1. For example, an age of 0.8 m.y. is assumed for Black Cone.
⁴ Crater Flat volcanoes are assumed to vary in age between 1.2 and 0.8 m.y.

frequency during t . In a time-truncated series, β and θ are estimated from the distribution of past events. In this case there are $n = 8$ new volcanoes formed in the YMR during the Quaternary. β and θ are given by:¹²

$$\beta = \frac{n}{\sum_{i=1}^n \ln\left(\frac{t}{t_i}\right)} \quad (3)$$

and

$$\theta = \frac{t}{n^{1/\beta}} \quad (4)$$

where t_i refers to the time of formation of the i th volcano. If β is approximately equal to unity, there is little or no change in the recurrence rate as a function of time and a homogeneous Poisson model would provide an estimate of regional recurrence rate quite similar to the nonhomogeneous Weibull-Poisson model. If $\beta > 1$ then a time trend exists in the recurrence rate and volcanoes form more frequently with time (i.e., waxing). If $\beta < 1$, new volcanoes form less frequently over time (i.e., waning).

Where few data are available, such as for volcanism in the YMR, the value of β can be strongly dependent on the period t and the timing of individual eruptions. Ho¹² analyzed volcanism from 6 Ma, 3.7 Ma, and 1.6 Ma to the present and concluded that volcanism is developing in the YMR on time scales of $t = 6$ Ma and 3.7 Ma, and has been relatively steady ($\beta = 1.1$) during the Quaternary.

Uncertainty in the ages of Quaternary volcanoes has a strong impact on recurrence rate estimates calculated using a Weibull-Poisson model. For example, if mean ages of Quaternary volcanoes are used (Table 1) and $t = 1.6$ Ma then, as Ho¹² calculated, $\beta = 1.1$ and the probability of a new volcano forming in the region within the next 10,000 yr is approximately 5%. This agrees well with recurrence rate

calculations based on simply averaging the number of new volcanoes that have formed since 1.6 Ma. However, if older volcano ages are used (i.e., Crater Flat volcanoes are 1.6 Ma) then $\beta = 0.3$ and the magmatic system appears to be waning. Using these parameters, the probability of a new volcano forming during a 10,000 yr confinement period is approximately 1.5% (Table 2). Conversely, if the Crater Flat volcanoes are only 0.8 Ma, the magmatic system appears to be waxing ($\beta = 2.2$) and the probability of a new volcano forming within 10,000 yr is approximately 10%. Therefore, given the uncertainty in the ages of Quaternary volcanoes in the YMR, it is currently not possible to differentiate between waxing and waning models for the frequency of new volcano formation using the Weibull-Poisson method over a constant time period, $t = 1.6$ Ma.

B. M. Crowe (written communication, 1993) has pointed out that the Weibull-Poisson model is strongly dependent on the value of t , and suggested that t should be limited to the time since the initiation of a particular episode of volcanic activity. This has an important effect on Weibull-Poisson probability models. If mean ages of Quaternary volcanoes are used and $t = 1.2$ Ma, the probability of a new volcano forming in the next 10,000 years drops from 5% to 2% and $\beta < 1$, indicating waning activity (Table 2). Alternatively, volcanism along the Crater Flat volcano alignment may have occurred over a period of several hundred thousand years.¹⁸ If volcanism was initiated along the alignment at approximately 1.2 Ma but continued through 0.8 Ma, the expected recurrence rate is again close to 5 v/my and the probability of new volcanism in the YMR within the next 10,000 yr is about 5% ($t = 1.2$ Ma, Table 2). The confidence intervals calculated on $\lambda(t)$ are quite large (Table 2) in all of these examples due to the few events ($n=8$) on which the calculations are based. Using the youngest volcano ages for example, the recurrence rate can only be constrained to less than 25 v/my with 90% confidence. Using mean ages, the recurrence rate is less than 12 v/my with 90 percent confidence (Table 2).

These calculations indicate that a broad range of expected regional recurrence rates should be considered in probability models primarily because of the few number of volcanic eruptions in the Quaternary and the relatively large uncertainty in the ages of these eruptions. Given this uncertainty, we adopt an estimate of 7 ± 3 v/my for the YMR,

with the understanding that additional high-precision dates may make it necessary to revise this estimate and that, currently, the 90% confidence envelopes for Weibull-Poisson recurrence rate distributions encompass a broader range of recurrence rates than are reflected in this estimate.

ESTIMATING SPATIAL VARIATION IN RECURRENCE RATE

Several models assessing the probability of future volcanic events in the YMR and the likelihood of a repository-disrupting event rely on the assumption that Plio-Quaternary vents have been emplaced in a completely spatially random (CSR) distribution over some bounded area.^{4,14-15} The assumption of a CSR, or spatially homogeneous Poisson distribution,¹⁹ of volcanoes does not seem appropriate because vents in the YMR appear to cluster, forming temporal and spatial patterns^{15,20} (Figure 1). This clustering is consistent with cinder cone clustering observed in other volcanic fields.²¹⁻²⁵ Sheridan²⁰ suggests that one method of accounting for spatial heterogeneity in vent distribution is to assume that post 4.5-Ma vents in Crater Flat system are formed as a result of steady-state activity, and that the dispersion of these vents represents two standard deviations on an elliptical Gaussian probability surface. Using this assumption, Sheridan²⁰ modeled the probability of repository disruption by Monte Carlo simulation for both volcanic events and dike intrusions, noting that variations in the shape of the probability surface significantly alter the probability of igneous disruption of the HLW repository. An alternative approach has been to define specific areas in which the recurrence rate of igneous events is increased. For example, Smith et al.²⁶ and Ho¹¹ define narrow NNE-trending zones within which average recurrence rate exceeds that of the surrounding region. These zones correspond to cinder cone alignment orientations that are presumably controlled by crustal structures.^{11,26}

Here, we apply two statistical tests to evaluate the null hypothesis that vents in the YMR are well described as CSR. One such test is the Clark-Evans, *CE*, test,²⁷ which compares the mean distance between nearest-neighbor observations, d , for n volcanoes within an area, A , against the mean distance, δ , expected from randomly distributed points within the same area:

$$CE = \frac{d - \delta}{s_e} \quad (5)$$

Assuming a spatially homogeneous Poisson distribution:²⁸

$$\delta = 0.5\sqrt{A/n}$$

and

$$s_e = \sqrt{\frac{0.0683A}{n^2}}$$

where s_e is the standard error. Applying the Clark-Evans test using all volcanoes within the AMRV (Figure 1 and Table 1), $n = 19$ volcanoes, $A = 1900 \text{ km}^2$, $d = 4200 \text{ m}$, $\delta = 5000 \text{ m}$, and $CE = -1.3$. Testing *CE* against a normal distribution rejects the null hypothesis at the 90% confidence level. Applying the test only to Quaternary volcanoes in the AMRV rejects the null hypothesis at a lower confidence level of 84%. However, the Clark-Evans test is not always robust because of

edge effects.²⁷⁻²⁹ In the YMR, for example, the ability to distinguish vent clusters from a CSR vent distribution is strongly dependent on the size and shape of the area considered. The AMRV is a minimum area bounding all volcanoes in the YMR less than $\approx 4.5 \text{ Ma}$ (Figure 1). It is less likely that the Clark-Evans test will identify clusters within this area than in a slightly larger area.

More recently, near-neighbor statistics have been developed to test for CSR distributions in point patterns (i.e., volcano distributions). Aherne and Diggle³⁰ define two measures of intensity (expected number of vents/unit area):

$$\lambda_p = \frac{m}{\sum_{i=1}^m u_i} \quad (6a)$$

$$\lambda_v = \frac{m}{\sum_{i=1}^m v_i} \quad (6b)$$

where u_i and v_i are areas of circles whose radii are the distance from the i^{th} randomly chosen point to the nearest volcano, and the i^{th} volcano to its nearest neighbor, respectively; m is the number of near neighbors; λ_p is the intensity estimated from m point-to-volcano measurements; and λ_v is the intensity estimated from m volcano-to-volcano measurements. For a CSR distribution, λ_p and λ_v should be approximately equal. In clustered distributions, λ_v tends to measure the intensity within clusters, and λ_p is a measure of cluster intensity.²⁸ The Hopkins *F*-test provides a method of testing for randomness in the vent pattern given these two measures of intensity:

$$Hop_F = \frac{\lambda_p}{\lambda_v} \quad (7)$$

The Hopkins *F*-test has a $F(2m, 2m)$ distribution.³¹ Following Aherne and Diggle,³⁰ random points within the AMRV are used to calculate λ_p . Considering all volcanoes in the AMRV: $\lambda_v = 3.85 \times 10^{-3}$ volcanoes/ km^2 , $\lambda_p = 9.31 \times 10^{-3}$ volcanoes/ km^2 , and $Hop_F = 2.42$. Considering only Quaternary volcanoes, $Hop_F = 3.14$. In either case, the null hypothesis that volcanoes are randomly distributed in the AMRV is rejected with greater than 99% confidence. Even in areas as narrowly defined as the CFVZ (Figure 1), the Hopkins *F*-test demonstrates with greater than 95% confidence that volcano distribution is not appropriately modeled as a CSR distribution. Using a paired Student *t*-test at a 99% confidence interval, the differences in ages of near-neighbor cinder cones is less than expected given a random distribution of ages, indicating that cinder cone clusters are temporally as well as spatially distinct.

Expected recurrence rate per unit area at an arbitrary point within the YMR also can be estimated using varying numbers of near neighbors:

$$\lambda_r = \frac{m}{\sum_{i=1}^m u_i^r} \quad (8)$$

where near-neighbor volcanoes are determined as the minimum of $u_i t_i$, and t_i is the time elapsed since the formation of the i^{th} near-neighbor volcano and u_i is defined as before, with $u_i \geq 1 \text{ km}^2$. We differentiate between various near-neighbor nonhomogeneous Poisson models by comparing the observed recurrence rate for the region with the expected regional recurrence rate calculated using near-neighbor methods, defined by:

$$\lambda_t = \iint_{\chi} \lambda_r(x, y) dy dx \quad (9)$$

where λ_t is the estimated YMR recurrence rate, based on the nonhomogeneous model. In practice, recurrence rates, λ_r , are calculated on a grid and these values are summed over the region of interest:

$$\lambda_t = \sum_{i=0}^m \sum_{j=0}^n \lambda_r(i, j) \Delta x \Delta y \quad (10)$$

where Δx and Δy are 2000 m, the grid spacing used in the calculations, and m and n are the number of grid points used in the X and Y directions, respectively. The dependence of expected regional recurrence rate, λ_t , on the number of near-neighbor volcanoes, m , used in the calculation is illustrated in Figure 2. The relationship between the number of near-neighbor volcanoes and regional recurrence rate depends on the ages of the volcanoes (equation 8), which are known with varying precision. Consequently, equation 10 is used to calculate regional recurrence rates using mean volcano ages, and the youngest and oldest ages for each volcano (Table 1) based on reported uncertainties in ages.^{4-6,32} Nonhomogeneous Poisson models using six to seven near-neighbor volcanoes give regional recurrence rates of 7 ± 3 v/my (Figure 2).

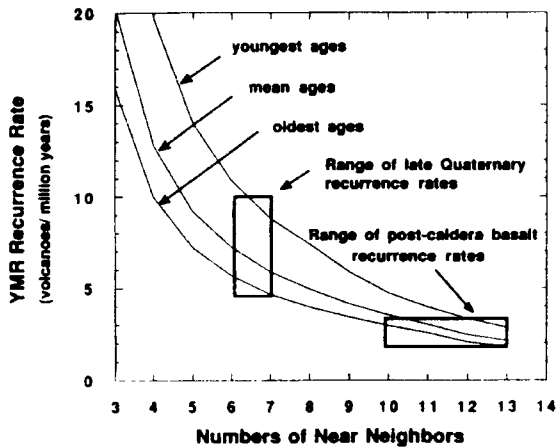


Figure 2: Recurrence rate for the formation of new volcanoes in the YMR is estimated using a number of near-neighbor nonhomogeneous Poisson models. Curves are calculated using mean volcano ages, oldest estimated ages, and youngest estimated ages (Table 1). Comparison with recurrence rates estimated directly from geochronological data indicates that six and seven near-neighbor models most closely approximate Quaternary recurrence rates; ten to thirteen near-neighbor models most closely approximate post-caldera basalt recurrence rates.

PROBABILITY MODELS

The probability of volcanic disruption of the candidate repository site can be estimated assuming a nonhomogeneous Poisson distribution

$$P[N(t) \geq 1] = 1 - \exp\left[-t \iint_{\chi} \lambda_r(x, y) dy dx\right] \quad (11)$$

where the limits of integration define the area of the repository. This relation is closely approximated in discretized form:

$$P[N(t) \geq 1] = 1 - \exp\left[-t \sum_a \lambda_r \Delta x \Delta y\right] \quad (12)$$

where Δx and Δy each are one kilometer and a is the approximate total area of the repository. These probabilities are very close to the probability of one volcanic event because the probability of two or more events is vanishingly small ($\approx 1 \times 10^{-9}$). The probabilities of volcanic disruption of the repository using a range of near-neighbor models are given in Figure 3. The probability of disruption also is determined for various repository areas calculated using mean volcano ages (Figure 4). The area of the HLW repository is currently estimated to be approximately 6 km^2 . Larger areas (i.e., 8 to 10 km^2) are presented to indicate the effects of an increase in repository size, and more importantly, to account for the area affected by the emplacement of a new volcanic center. Scoria mounds and related satellite vents at Red Cone, Black Cone, and Lathrop Wells^{26,33} extend for at least 0.5 km around the main vent, which indicates that establishing a new volcanic center within roughly 0.5 km of the repository may result in direct disruption of the HLW repository. An area of 8 to 10

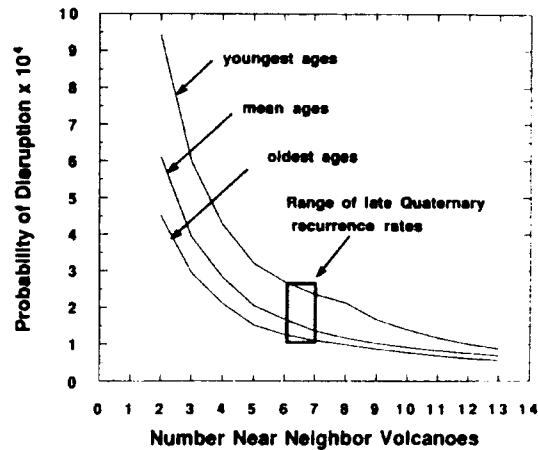


Figure 3: Estimated probability of disruption of the HLW repository varies with the number of near neighbors used in nonhomogeneous Poisson models and with the uncertainty in the ages of Quaternary YMR cinder cones (Table 1). Calculations are made for the probability of a volcano forming within an 8 km^2 block at the candidate repository site (Figure 1) during the next 10,000 years. Six to seven near-neighbor models most closely approximate a Quaternary recurrence rate of 7 ± 3 v/my. Ten to thirteen near-neighbor models most closely approximate a post-caldera basalt recurrence rate of 3 v/my.

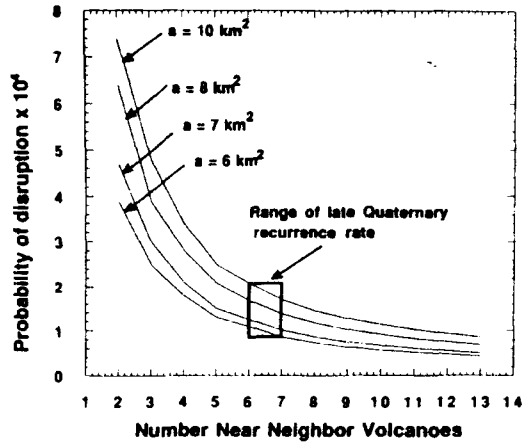


Figure 4: Estimated probability of a volcano forming at the repository site (Figure 1) increases with increasing area of the site. Magma erupting at main vents located outside the repository perimeter may disrupt the repository, as cinder cones in the region often have satellite vents that extend to 0.5 km. Larger area calculations (e.g., $a = 10 \text{ km}^2$) account for the probability of disruption by vents centered within 0.5 km of the repository. Calculations are made using mean volcano ages (Table 1) and indicate the probability of disruption during the next 10,000 years. Six to seven near-neighbor models most closely approximate the Quaternary recurrence rate. Ten to thirteen near-neighbor models most closely approximate the post-caldera basalt recurrence rate.

km^2 , therefore, may more accurately reflect the area within which a new volcanic center could form and disrupt the HLW repository. Using an 8 km^2 area in equation 12, the probability of disruption during a 10,000 year confining period is between 1.4×10^{-4} and 1.7×10^{-4} for a mean late-Quaternary recurrence rate (six to seven near-neighbors) and 6.9×10^{-5} to 9.2×10^{-5} for a post-caldera basalt recurrence rate (ten to thirteen near-neighbors). Using a range of Quaternary rates ($7 \pm 3 \text{ v/my}$) and an 8 km^2 area, the probability of disruption is between 1.1×10^{-4} and 2.7×10^{-4} . For a larger area ($a = 10 \text{ km}^2$) and using young volcano ages, the probability of volcanic disruption in 10,000 years increases to 3.4×10^{-4} . Conversely, using the oldest ages for volcanoes and a smaller area, $a = 6 \text{ km}^2$, the probability of disruption is 8.0×10^{-5} . Based on the nonhomogeneous Poisson models for various Quaternary recurrence rates and areas, most estimates of the probability of repository disruption are between 1×10^{-4} and 3×10^{-4} for the next 10,000 years (Figures 3 and 4).

One way to illustrate spatial variation in estimated recurrence rate for the YMR, and hence the probability of disruptive volcanic events, is to map probabilities calculated from nonhomogeneous Poisson models. Applying equation 8, the expected recurrence rate is estimated at points on a grid (grid node spacing 2 km) using different numbers of near-neighbors. Probabilities of at least one event occurring within one repository area (8 km^2) about each grid point during the next 10,000 years are then calculated (equation 12). Two such maps are illustrated in Figures 5a and 5b, generated using six and eleven near-neighbors, respectively. The tendency for vents to cluster is well illustrated by the $m = 6$ near-neighbors

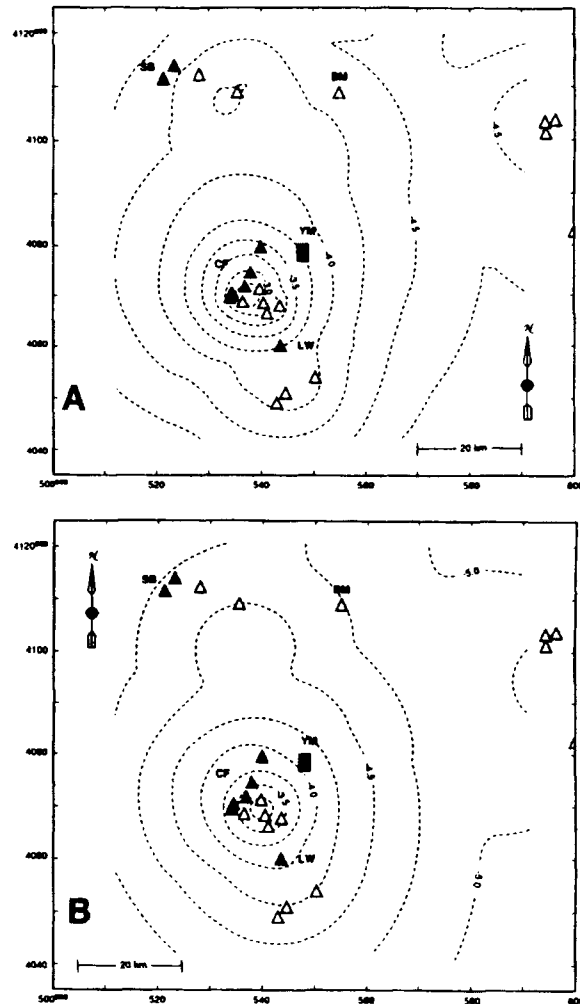


Figure 5: Probability of a new volcano forming during the next 10,000 years varies in the YMR because of the tendency for volcanoes to cluster. Here the logarithm of probability of a volcano forming within a 8 km^2 area during the next 10,000 years is contoured using 6 near-neighbor (a) and 11 near-neighbor (b) nonhomogeneous Poisson models. These models reflect Quaternary and post-caldera basalt recurrence rates, respectively. Both models indicate that the probability of disruption of the proposed repository (solid rectangle) is higher than in the YMR as a whole due to the relative proximity of the site to Quaternary Crater Flat volcanoes. Solid triangles are Quaternary volcanoes, open triangles are Neogene vents, YM - Yucca Mountain repository, CF - Crater Flat, SB - the Sleeping Butte volcanoes (Little Black Peak and Hidden Cone), BM - Buckboard Mesa, and LW - Lathrop Wells (Table 1). The contour interval is $0.25 \log(P[N \geq 1, 10,000 \text{ yr}])$ (e.g., -4 is a probability of 1×10^{-4} of a new volcano forming within an 8 km^2 area in 10,000 years). Across the YMR, probabilities vary from more than 1×10^{-3} in Crater Flat Valley (Figure 5a) to less than 1×10^{-5} . Map coordinates are in Universal Transverse Mercator, Clarke 1866 projection.

probability map. On this map (Figure 5a), the probability of renewed volcanic activity is highest in Crater Flat. South of Red Cone, for example, the probability of a new volcanic center forming in the next 10,000 years within an 8 km² area is between 1.6×10^{-3} and 2.0×10^{-3} for a mean Quaternary recurrence rate (i.e., six to seven near-neighbors) and between 2.0×10^{-4} and 8.0×10^{-4} for a post-caldera basalt recurrence rate (i.e., ten to thirteen near-neighbors). Probability contours are elongate in a N-S direction, reflecting the overall distribution of Quaternary cones. Although the probability of disruption is less using an $m = 11$ near-neighbor model (Figure 5b), the Crater Flat cluster persists as an area of high probability on this plot and probability contours remain elongate in a N-S direction. In all cases, the probability of volcanic disruption of the proposed HLW repository is high compared with most homogeneous Poisson models^{4,14-15} because the repository site is relatively close to the largest cluster of young volcanoes in the YMR.

SUMMARY OF PROBABILITY ANALYSIS

Probability models based on the assumption of complete spatial randomness will overestimate the likelihood of future igneous activity in parts of the YMR far from Quaternary centers and underestimate the likelihood of future igneous activity within and close to Quaternary volcano clusters (Figures 5a and 5b). This has a profound influence on probability calculations for future igneous activity near the candidate HLW repository, because the site is located comparatively close to Crater Flat, the largest cluster of young volcanoes in the YMR (Figure 1). Vent clustering in the YMR is statistically significant, and robust probability models should account for this clustering. Nonhomogeneous Poisson probability models calculated by near-neighbor methods can be used to estimate the probability of volcanic disruption of the candidate HLW repository. Assuming a Quaternary recurrence rate of 7 ± 3 v/my, these models estimate a probability of disruption between 8.0×10^{-5} and 3.4×10^{-4} in 10,000 years, with most estimates between 1×10^{-4} and 3×10^{-4} . The candidate HLW repository site is positioned on a probability gradient. West of the proposed site, the probability of volcanism within the next 10,000 years increases substantially due to the presence of Quaternary volcanoes in Crater Flat. The probability of volcanism within the next 10,000 years decreases east of the proposed repository site. Further refinement of probability models will likely alter these estimates, and they are not intended to represent a complete analysis of the probability of repository disruption by igneous activity. The proposed nonhomogeneous model takes into account one important geological feature of volcanic fields: centers tend to cluster within these fields through time. Additional geological information, such as the impact of pre-existing structure²⁶ or strain rate on volcanism, will need to be fully taken into account before a more refined assessment of the probability of future volcanic activity in the YMR can be made with confidence.

ACKNOWLEDGMENTS

Budhi Sagar, William M. Murphy, Gerry L. Stirewalt, and Kenneth D. Mahrer provided comprehensive reviews of this work. This manuscript was prepared to document work performed at the Center for Nuclear Waste Regulatory Analyses (CNWRA) for the U.S. Nuclear Regulatory Commission (NRC) under Contract No. NRC-02-88-005. The activities reported herein were performed on behalf of the NRC Office of Nuclear Regulatory Research. This report is an independent product of the CNWRA and does not necessarily reflect the views or regulatory position of the NRC.

REFERENCES

1. Crowe, B.M., K.H. Wohletz, D.T. Vaniman, E. Gladney, and N. Bower. *Status of Volcanic Hazard Studies for the Nevada Nuclear Waste Storage Investigations*. LA-9325-MS, Vol. II. Los Alamos National Laboratory (1986).
2. Vaniman, D.T., B.M. Crowe, and E.S. Gladney. Petrology and geochemistry of Hawaiiite lavas from Crater Flat, Nevada. *Contributions in Mineralogy and Petrology* 80: 341-357 (1982).
3. Crowe, B.M. Basaltic volcanic episodes of the Yucca Mountain region. High-Level Radioactive Waste Management, International Conference, April 8-12, 1990, Las Vegas, Nevada. *American Nuclear Society* 1:65-73 (1990).
4. Crowe, B.M., M.E. Johnson, and R.J. Beckman. Calculation of the probability of volcanic disruption of a high-level nuclear waste repository within southern Nevada, USA. *Radioactive Waste Management and the Nuclear Fuel Cycle* 3:167-190 (1982).
5. Vaniman, D.T., and B.M. Crowe. *Geology and Petrology of the Basalts of Crater Flat: Applications to Volcanic Risk Assessment for the Nuclear Waste Storage Investigations*. LA-8845-MS. Los Alamos National Laboratory (1981).
6. Crowe, B.M., S. Self, D.T. Vaniman, R. Amos, and F. Perry. Aspects of potential magmatic disruption of a high-level nuclear waste repository in southern Nevada. *Journal of Geology* 91: 259-276 (1983).
7. Turrin, B.D., and D.E. Champion. ⁴⁰Ar/³⁹Ar laser fusion and K-Ar ages from Lathrop Wells, Nevada, and Cima, California: the age of the latest volcanic activity in the Yucca Mountain area. Proceedings of the Second International Conference on High-Level Radioactive Waste Management, LaGrange Park, IL. *American Nuclear Society* 2: 68-75 (1991).
8. Turrin, B.D., D. Champion, and R.J. Fleck. ⁴⁰Ar/³⁹Ar age of the Lathrop Wells volcanic center, Yucca Mountain, Nevada. *Science* 253: 654-657 (1991).
9. Crowe, B., R. Morley, S. Wells, J. Geissman, E. McDonald, L. McFadden, F. Perry, M. Murrell, J. Poths, and S. Forman. The Lathrop Wells volcanic center: Status of field and geochronology studies. Proceedings of the Third International High Level Radioactive Waste Management Conference. La Grange Park, IL. *American Nuclear Society*. 2:1,997-2,013 (1992).
10. Poths, J., and Crowe, B.M. Surface exposure ages and noble gas components of volcanic units at the Lathrop Wells volcanic center, Nevada. *Eos, Transactions of the American Geophysical Union* 73: 610 (1992).
11. Ho, C.-H. Risk assessment for the Yucca Mountain high-level nuclear waste repository site: estimation of volcanic disruption. *Mathematical Geology* 24: 347-364 (1992).
12. Ho, C.-H., Time trend analysis of basaltic volcanism at the Yucca Mountain site. *Journal of Volcanology and Geothermal Research* 46:61-72 (1991).
13. Ho, C.-H., E.I. Smith, D.L. Feurbach, and T.R. Naumann. Eruptive probability calculation for the Yucca Mountain site, USA: statistical estimation of recurrence rates. *Bulletin of Volcanology* 54:50-56 (1991).